Journal of Molecular Structure 1060 (2014) 42–48

Contents lists available at ScienceDirect

Journal of Molecular Structure

journal homepage: www.elsevier.com/locate/molstruc

A zinc(II) quinolinone complex $(Et_3NH)[Zn(qui)Cl_2]$: Synthesis, X-ray structure, spectral properties and *in vitro* cytotoxicity

Roman Buchtík [a], Ivan Nemec [b], Zdeněk Trávníček [b,*]

[a] Department of Inorganic Chemistry, Faculty of Science, Palacký University, 17. listopadu 12, CZ-771 46 Olomouc, Czech Republic
[b] Regional Centre of Advanced Technologies and Materials, Department of Inorganic Chemistry, Faculty of Science, Palacký University, 17. listopadu 12, CZ-77146 Olomouc, Czech Republic

HIGHLIGHTS

- The first zinc(II) quinolinone complex was synthesized and characterized.
- The compound is composed of triethylammonium cation and $[Zn(qui)Cl_2]$ anion.
- Secondary structure shows a *zig–zag* 1D supramolecular architecture.
- The fluorescence of the complex is enhanced as compared to free H*qui* ligand.
- The compound displays no relevant *in vitro* cytotoxicity against HOS and MCF7.

GRAPHICAL ABSTRACT

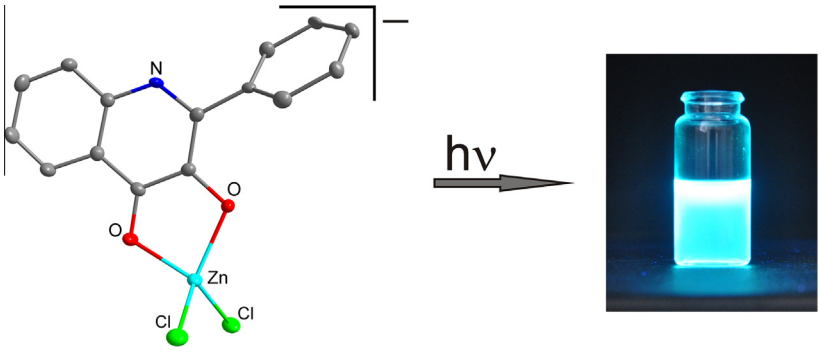

ARTICLE INFO

Article history:
Received 10 September 2013
Received in revised form 2 December 2013
Accepted 4 December 2013
Available online 22 December 2013

Keywords:
Zinc(II) complex
Quinolinone
NMR spectroscopy
X-ray structure
Fluorescence
In vitro cytotoxicity

ABSTRACT

A new zinc(II) complex with 2-phenyl-3-hydroxy-4(1*H*)-quinolinone (H*qui*) of the composition $(Et_3NH)[Zn(qui)Cl_2]$ was prepared and characterized by elemental analysis, FT IR, 1D and 2D NMR, and fluorescence spectroscopy, mass spectrometry and single crystal X-ray analysis. The molecular structure is composed of the triethylammonium (Et_3NH^+) cations and tetrahedral $[Zn^{II}(qui)Cl_2]^-$ complex anions, in which the Zn(II) atoms are bidentate coordinated by one *qui* ligand through keto (O_K) and phenolate (O_P) oxygen atoms and by two chlorido ligands, thus forming the $\{O_2Cl_2\}$ donor set, with Zn–O_K = 1.9860(14) Å, Zn–O_P 1.9961(14) Å and Zn–Cl = 2.2509(6) Å and 2.2266(6) Å. The complex cations are aligned into 1D supramolecular chains through the N—H···Cl hydrogen bonding between the amine group of the quinolinone ligand and the chlorido ligand of the adjacent complex anion. The amine group from the Et_3NH^+ cations provides the N—H···O_P hydrogen bond with the phenolate oxygen atoms from the complex anion. Screening of *in vitro* cytotoxicity of the compound was studied on human osteosarcoma (HOS) and human breast adenocarcinoma (MCF7) cell lines, with IC_{50} > 50 μM. The fluorescence study showed that the complex exhibits a relatively high integral intensity (29%) as compared to the standard quinine sulfate, and 1.6-fold enhancement of emission with respect to free H*qui*.

1. Introduction

In a few past decades, there have been performed massive investigations in cytotoxicity and genotoxicity of new metal-based antitumor complexes able to overcome *cisplatin* resistance and its high toxicity in the field of medicinal and bioinorganic chemistry. The chemists and drug designers have focused their interests on the preparation and study of a number of transition metal complexes other than platinum, which could offer unique properties such as variable redox states, photoluminescence properties and ability of targeting DNA through non-covalent modes of action [1–6]. In an attempt to obtain non-platinum based biologically active complexes, which would exceed anticancer effect and concurrently reduce

* Corresponding author. Tel.: +420 585 634 352; fax: +420 585 634 954.
E-mail address: zdenek.travnicek@upol.cz (Z. Trávníček).

0022-2860/$ - see front matter © 2013 Elsevier B.V. All rights reserved.
http://dx.doi.org/10.1016/j.molstruc.2013.12.050

toxicity in comparison with clinically-used *cisplatin*, we recently published mixed-ligand copper(II) complexes, involving 2-phenyl-3-hydroxy-4(1*H*)-quinolinone (H*qui*) and its derivatives, of a general composition [Cu(qui)(Nlig)]X (Nlig = derivatives of 1,10-phenanthroline or 2,2′-bipyridine, X = BF_4 or NO_3). These complexes showed significantly higher anticancer effect against a series of human cancer cell lines together with reduced toxicity against healthy human cells as compared to *cisplatin* indeed [7–9]. The highest cytotoxicity was found for the complexes [Cu(qui)(mphen)]BF_4·H_2O (IC_{50} = 0.36 μM and 0.56 μM), [Cu(qui)(bphen)]NO_3·H_2O (IC_{50} = 0.66 μM and 0.73 μM) and [Cu(qui)(bphen)]BF_4 (IC_{50} = 0.57 μM and 0.70 μM) (where mphen = 5-methyl-1,10-phenanthroline and bphen = bathophenanthroline) against A2780 (ovarian carcinoma), and A2780cis (*cisplatin*-resistant ovarian carcinoma) respectively, as compared with the values of 12.0 μM, and 27.0 μM determined for *cisplatin*.

The originally anticancer inactive H*qui* used as a ligand in the above mentioned and highly cytotoxic Cu(II) complexes belongs to a vast group of quinolinones which are otherwise generally known not only for a number of biological activities e.g. cytotoxicity [10–12] but they are also characteristic for their intrinsic photoluminescence [13,14]. Photoluminescence effects, such as fluorescence could be contributive in the study of cytotoxic compounds, because these physical properties could e.g. enable a detailed investigation of their possible interaction with DNA through several spectral methods, suggesting partial inter-base intercalations or other non-covalent DNA interactions [15]. In this context, the preparation of Zn(II) complexes with the quinolinones represents the next logical step in our ongoing studies of these organic compounds as ligands in transition metal complexes, for multiple reasons: (a) zinc belongs among the most abundant metals in human body, and plays an irreplaceable role in loads of biological processes such as enzymatic regulation [16,17], neural signal transmission [18,19] and also DNA binding [20]; (b) Zn(II) complexes frequently exhibit fluorescence and moreover have often been observed to have higher intensity in comparison with the parent organic compound due to enhancement of the charge-transfer character of the excited state of the chromophore [21,22]; and (c) additionally, in the last decade, there has been a number of studies on cytotoxicity of Zn(II) complexes, where such compounds have been found significantly active [23–25], and in particular, selective against prostatic tumor cells, e.g. Zn(II) complexes with thiosemicarbazones of a general composition [Zn(bpy)(L_1)], where bpy = 2,2′-bipyridine and L_1 stands for substituted semicarbazones. The significant cytotoxicity against the prostate cancer cell line (PC3) was found e.g. for [Zn(bpy)(HP)]·$2H_2O$ (IC_{50} = 0.84 μM), where HP = 4-hydroxysalicylaldiminato-4′-phenylthiosemicarbazone [26]. Another group of zinc complexes showing considerable activity against PC3 is that of a general composition [Zn(bpy-9)(L_2)$_2$], where bpy-9 = 4,4′-dinonyl-2,2′-bipyridine and L_2 stands for a diketonate such as tropoloid. The complex exhibiting the highest cytotoxicity was [Zn(bpy-9)(QT)$_2$] (IC_{50} = 2.8 μM), where QT = 4-(3,3-dimethylbutanoyl)-5-methyl-2-phenyl-1*H*-pyrazol-3-one [27].

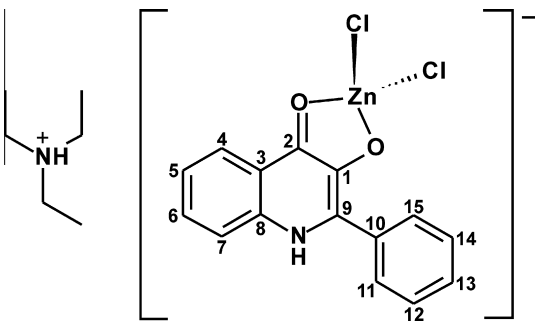

Scheme 1. Structural formula of (Et_3NH) [Zn(*qui*)Cl_2] together with the atom numbering.

Herein, we present the preparation, solid-state and solution characterizations, and *in vitro* antitumor screening for (Et_3NH)[Zn(*qui*)Cl_2] (Scheme 1). This compound was studied primarily due to its possible potential to combine cytotoxic and luminescent properties and furthermore, the Zn(II) compounds with the quinolinone derivatives have also never been studied and structurally characterized yet. (Cambridge Crystallographical Database (CSD), ver. 5.34, May 2013 update).

2. Experimental

2.1. Materials and methods

Chemicals and solvents were purchased from Sigma–Aldrich Co. and Acros Organics Co., and were used as received. 2-Phenyl-3-hydroxy-4(1*H*)-quinolinone (H*qui*) was synthesized following the formerly reported procedure [28] in a high yield (>95%). The compound was characterized by elemental analysis, FT IR and also single crystal X-ray analysis [7]. Anal. Calcd for $C_{15}H_{11}NO_2$ (M = 237.3 g mol^{-1}) (%): C, 75.9; H, 4.7; N, 5.9. Found: C, 75.6; H, 4.3; N, 5.7. FT IR (ν_{ATR}/cm^{-1}): 518w, 644w, 693m, 707m, 758s, 842w, 909w, 995m, 1030m, 1150m, 1267vs, 1368vs, 1403s, 1489s, 1550s ν(C=C$_{arom}$), 1631vs ν(C=O).

Elemental analyses (C, H, N) were performed on a Flash 2000 CHNO-S Analyser (Thermo Scientific). Conductivity measurements were carried out on a Cond 340i/SET (WTW) in nitromethane 10^{-3} M solution at 25 °C. Electronic absorption spectra of 10^{-4} M ethanolic and/or 0.1 M H_2SO_4 solutions were recorded with a Lambda 40 spectrometer (Perkin Elmer instruments) in the range of 200–1000 nm. Mass spectrometry studies were performed on an LTQ Fleet (ThermoFisher Scientific) with the ESI-(negative-ion electrospray ionization) full scan mode in 10^{-5} M methanolic solutions. FT IR spectra were recorded on a Nexus 670 FT IR (ThermoNicolet) using the ATR technique in the range of 200–4000 cm^{-1}. The intensities of reported FT IR signals are defined as vs = very strong, s = strong, m = medium, w = weak and br = broad. ^1H and ^{13}C NMR spectra and 2D correlation experiments (^1H—^1H gs-COSY, ^1H—^{13}C gs-HMQC and ^1H—^{13}C gs-HMBC; gs = gradient selected, COSY = correlation spectroscopy, HMQC = heteronuclear multiple quantum coherence and HMBC = heteronuclear multiple bond coherence) of the DMF-d_7 solutions were measured at 300 K on a Varian 400 device (Varian, Santa Clara, CA, USA) at 400.00 MHz (^1H) and 100.58 MHz (^{13}C). The spectra were adjusted against the tetramethylsilane (TMS) signals and calibrated against the residual signals of the DMF adjusted to 8.03 ppm (^1H) and 162.3 ppm (^{13}C). The splitting of proton resonances in the reported ^1H spectra is defined as s = singlet, d = doublet, t = triplet, q = quartet, br = broad band, m = multiplet. Fluorescence solution spectra were recorded on an AvaSpec HS1024x122TE spectrometer using 0.5 cm cuvettes at room temperature. The fluorescence relative integral intensity of (Et_3NH) [Zn(*qui*)Cl_2] and ligand H*qui* were determined in 10^{-4} M ethanolic solutions by a comparison with the fluorescence of quinine sulfate as a reference fluorescence standard (10^{-4} M solution of the standard in 0.1 M sulfuric acid in ethanol) [29]. The measured compounds were excited at the wavelengths of absorption maximum of each compound.

X-ray experiment of a selected crystal of (Et_3NH) [Zn(*qui*)Cl_2] was collected on an Xcalibur™2 diffractometer (Oxford Diffraction Ltd.) with the Sapphire2 CCD detector, and with Mo Kα radiation (Monochromator Enhance, Oxford Diffraction Ltd.). Data collection and reduction were performed using the CrysAlis software [30]. The structure was solved by direct methods using SHELXS-97 and

refined on F^2 using the full-matrix least-squares procedure (SHELXL-97) [31]. Non-hydrogen atoms were refined anisotropically and hydrogen atoms were located in difference Fourier maps and refined by using the riding model, with C—H = 0.95, 0.98 and 0.99 Å, N—H = 0.88 and 0.93 Å, and with $U_{iso}(H) = 1.2U_{eq}$ (CH, CH_2, NH) and $U_{iso}(H) = 1.5U_{eq}$ (CH_3). The crystal data and structure refinements are given in Table 1. The molecular graphics as well as additional structural calculations were drawn using DIAMOND [32].

2.2. Synthesis

The starting ligand H*qui* (2 mmol; 474 mg) was dissolved in 50 mL of hot ethanol and then Et_3N (2 mmol; 275 μL) was slowly added. To this mixture, a 10 mL of ethanolic solution of $ZnCl_2$ (2 mmol; 270 mg) was added and refluxed for 1 h. After cooling down, the solution was filtered and left to stand at ambient temperature. Within two days, golden-yellow crystals of product started to form. The crystals were filtered off and dried at 40 °C under an infrared lamp. Yield: 628 mg (66%). Anal. Calcd for $C_{21}H_{26}N_2Cl_2O_2Zn$ (M = 474.7 g mol^{-1}) (%): C, 53.1; H, 5.5; N, 5.9. Found: C, 53.5; H, 5.8; N, 5.5.

ESI–MS: *m/z* 236 ([*qui*]$^-$, 100%), 334 ([Zn(*qui*)Cl—H]$^-$, 18%), 372 ([Zn(*qui*)Cl_2]$^-$, 3%), 535 ([Zn(*qui*)$_2$—H]$^-$, 3%).

^{1}H NMR (DMF-d_7, TMS, δ ppm) *J* (Hz): 1.28, 9H, *t*, (7.2), CH_3; 3.24, 6H, *q*, (7.0), CH_2; 7.29, 1H, *t*, (7.6), HC^5; 7.42, 1H, *t*, (7.4) HC^{13}; 7.51, 3H, *m*, HC^{6,12,14}; 7.93, 1H, *d*, (8.6) HC^7; 8.24, 3H, *d*, (8.2), HC^{4,11,15}; 11.98, 1H, *br*, HN^1.

^{13}C NMR (d_7-DMF, TMS, δ ppm): 8.9 ($3C_{CH3}$), 46.7 ($3C_{CH2}$), 118.8 (C7), 119.5 (C3), 122.0 (C5), 124.2 (C4), 128.1 (C12, 14), 128.5 (C6), 129.1 (C13), 129.3 (C11, 15), 131.4 (C9), 134.5 (C10), 135.9 (C1), 149.7 (C8), 172.9 (C2).

FT IR (ν_{ATR}/cm^{-1}): 242w, 268s, 274s, 288vs, 291vs, 310s, 330w, 378m, 391w, 450s, 472s, 492w, 549m, 646m, 660m, 693m, 715m, 729m, 764s, 800m, 834w, 910w, 926w, 999m, 1034m, 1126m, 1153m, 1213s, 1264s, 1365vs, 1388s, 1447vs, 1464vs, 1486vs, 1519s, 1561s, 1579m, 1628s, 2497s, 2629s, 2828br, 2978vs, 3004vs, 3056vs, 3140vs, 3170vs, 3201vs, 3228vs, 3500br.

2.3. In vitro cytotoxicity

In vitro cytotoxicity of (Et_3NH) [Zn(*qui*)Cl_2] was determined by an MTT assay [MTT = 3-(4,5-dimethylthiazol-2-yl)-2,5-diphenyltetrazolium bromide] on human Caucasian osteosarcoma cells (HOS; ECACC No. 87070202) and human Caucasian breast adenocarcinoma cells (MCF7; ECACC No. 86012803). Human cancer cell lines were purchased from the European Collection of Cell Cultures (ECACC). The cells were cultured according to the manufacturer's instructions and maintained at 37 °C and 5% CO_2 in a humidified incubator (100% humidity).

The cancer cell lines were treated with the tested compounds for 24 h, using multi-well culture plates of 96 wells. The tested compound (Et_3NH)[Zn(*qui*)Cl_2] and *cisplatin* were applied to the cells at the concentrations of 0.01, 0.1, 1.0, 5.0, 25.0 and 50.0 μM. In parallel, the cells were treated with vehicle (DMF; 0.1% v/v) and Triton X-100 (1% v/v) to assess the minimal (i.e. positive control) and maximal (i.e. negative control) cell damage, respectively. Cells were incubated with MTT for 3–4 h, after removal of the medium and washing the cells with the phosphate buffer solution, formazan dye was dissolved in DMF containing 1% of ammonia. The MTT assay absorbance was measured spectrophotometrically at 540 nm (TECAN, Schoeller Instruments LLC). The data were expressed as the percentage of viability, when 100% and 0% represent the treatments with DMF, and Triton X-100, respectively. The data regarding the cancer cell lines were obtained from three independent cell passages. The obtained $IC_{50} \pm SD$ (μM) values together with their standard deviations were calculated from viability curves.

Table 1
Crystal data and structure refinement for (Et_3NH) [Zn(*qui*)Cl_2].

Formula	$C_{21}H_{26}Cl_2N_2O_2Zn$
Formula weight (g mol^{-1})	474.70
Crystal color	Yellow
Temperature (K)	150(2)
Wavelength (Å)	0.71073
Crystal system	Monoclinic
Space group	$P2_1/c$
a (Å)	12.0722(5)
b (Å)	9.7792(4)
c (Å)	18.7384(8)
α (°)	90
β (°)	101.685(4)
γ (°)	90
V (Å^3)	2166.34(16)
Z, ρ_{calc} /g cm^{-3}	4, 1.593
μ (mm^{-1})	1.399
F(000)	984
Final *R* indices	$R_1 = 0.0264$
[$I > 2\sigma(I)$]	$wR_2 = 0.0539$
R indices (all data)	$R_1 = 0.0402$
	$wR_2 = 0.0558$
GoF on F^2	0.903
CCDC Ref. no	959886

3. Results and discussion

3.1. General characterization

The (Et_3NH) [Zn(*qui*)Cl_2] compound was obtained in the form of pale golden-yellow crystals, while its purity, composition and structure were based on the results following mainly from elemental analysis, mass spectrometry, NMR data and X-ray analysis. The molar conductivity value of the studied complex dissolved in nitromethane equals 78.5 S cm^2 mol^{-1}, which fits in the 75–95 S cm^2 mol^{-1} range that is characteristic for the 1:1 electrolyte for this type of solvent [33].

3.2. X-ray crystallography

The studied compound (Et_3NH) [Zn(*qui*)Cl_2] consists of the tetrahedral complex anions [Zn^{II}(qui)Cl_2]$^-$ and triethylammonium (Et_3NH^+) cations (Fig. 1). The complex crystallizes as yellow planar crystals in the $P2_1/c$ space group (Table 1). The complex anions consist of one the *qui* ligand coordinated to the Zn(II) atom in a chelate manner through the keto (O_K) and phenolate (O_P) oxygen atoms, and two chlorido ligands thus forming the {ZnO_2Cl_2} chromophore with the tetracoordinated central Zn(II) atom (Fig. 1). The ZnO bond lengths are of a similar length with a bit shorter Zn—O_K bond (1.9860(14) Å) in comparison to ZnO_P (1.9961(14) Å). Two chloride anions act as terminal ligands, with *d*(ZnCl) = 2.2509(6) and 2.2266(6) Å. These chromophore bond lengths are comparable to those reported previously for similar systems (Table 2).

The chromophore angles are strongly affected by the chelating nature of the *qui* ligand, which induces the formation of a very narrow O_K—Zn—O_P angle (85.12(6)°, Table 2). The remaining OZnCl and ClZnCl angles are in the range of 108.7–117.6°, and such an angular distortion of the coordination polyhedron is typical for the tetrahedral complexes with chelating O,Oligands. As an example, the bite angles of complexes [Zn(*eaa*)Cl_2] and [Zn(*aed*)Cl_2] can be mentioned, in which the O—Zn—O angles adopt values of 87.52(7)°, and 88.4(2)°, respectively (*eaa* = N,N′-ethylene-acetylacetonimine, *aed* = (2-hydroxy-4-methoxy acetophenone)ethylenediamine) [37,38].

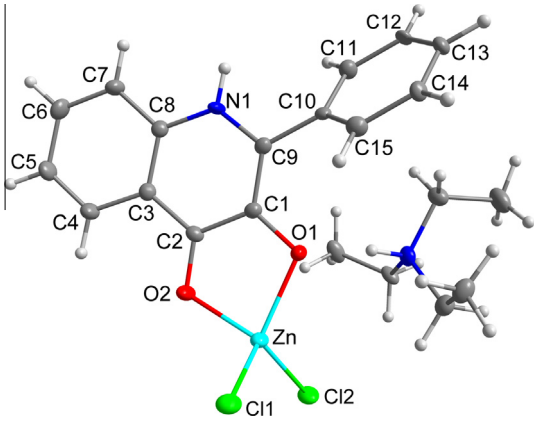

Fig. 1. Molecular structure of (Et_3NH) $[Zn(qui)Cl_2]$ together with the atom numbering scheme. The non-H atoms are drawn as thermal ellipsoids at the 50% probability level.

The *qui* ligand involves benzene and pyridine rings, which are nearly coplanar with the dihedral angle being 3.99(6)°, while the least-square planes fitted through the *qui* and phenyl moieties make a dihedral angle of 50.71(6)°.

The crystal structure of (Et_3NH) $[Zn(qui)Cl_2]$ is stabilized by a network of non-covalent contacts of the N—H···O, N—H···Cl, C—H···O and C—H···Cl types, and can be formally classified as one-dimensional due to a presence of chain sub-structures of the complex anions bonded together through the N—H···Cl hydrogen bonds (with the N···Cl distance of 3.255(2) Å) forming between the amine groups of the *qui* ligand and the chlorido ligands of the adjacent complex anions (Fig. 2, *top*). The Et_3NH^+ cations are in interactions with the complex anions by N—H···O_P hydrogen bonds of a moderate strength: d(N1A···O_P) = 2.773(2) Å (Fig. 2, *down left*). From the other non-covalent interactions presented in (Et_3NH) $[Zn(qui)Cl_2]$, the centrosymmetric pairs of C—H···O interactions between quinolinone aromatic CH groups and keto oxygen atoms has to be mentioned (a ring synthon $R_2^2(10)$, Fig. 2, *down right*): d(C···kO_K) = 3.462(3) Å. These contacts represent the most important non-covalent interconnections between the 1D chains of the complex anions in the crystal structure of (Et_3NH) $[Zn(qui)Cl_2]$.

3.3. Spectral properties of (Et_3NH) $[Zn(qui)Cl_2]$

The band of the characteristic ν(C⁼⁼O) vibration of the quinolinone moiety was observed in the FT IR spectrum of the complex at 1628 cm^{-1}, which might be surprising, because it does not differ markedly from that of the uncoordinated H*qui* found at 1631 cm^{-1}. Nevertheless, this phenomena has already been observed before in the case of Cu(II)-quinolinone complexes [7]. The bands centred at 3228 and 3201 cm^{-1} are assignable to the $(N—H)_{aromatic}$ stretching vibrations, while the bands at 3056 and 3140 cm^{-1} may be connected with $\nu(C—H)_{aromatic}$. The presence of the triethylammonium cation can be supported by the existence of bands at 2828, and 2497 and 2629 cm^{-1}, which may be attributable to the N—H protonated, and CH_2 and CH_3 vibrations, respectively [42]. The band belonging to the Zn—Cl stretchning vibration was observed at ca 290 cm^{-1} [43,44], while the band recorded at 450 cm^{-1} may be associated with ν(Zn–O) [45].

The mass spectrum of (Et_3NH) $[Zn(qui)Cl_2]$ was measured in the ESI-mode. The peak with m/z = 372 corresponds to the complex anion $[Zn(qui)Cl_2]^-$ with the characteristic zinc isotopic distribution. The peak with the 100% relative intensity observed at m/z = 236 represents the ligand $[qui]^-$. There are also two other fragments, the first observed at m/z = 334, corresponding to $[Zn(qui)Cl—H]^-$, and the next one detected at m/z = 535 assignable to $[Zn(qui)_2—H]^-$ species (Fig. 3).

The composition of (Et_3NH) $[Zn(qui)Cl_2]$ was assigned through a detailed data analysis of ^1H and ^{13}C NMR experiments. The protons at aliphatic trimethylammonium and aromatic rings carbons were assigned by their chemical shifts δ (ppm) and multiplicity. The signals in the ^1H NMR spectrum showed a very high purity (>98%) of the measured compound. The ^1H NMR spectra contain the triplet and quartet at 1.28, and 3.24 ppm, respectively, belonging to the three CH_3— groups and three CH_2— groups of the triethylammonium cation. The peaks in the range of 7.29–8.24 ppm correspond to the eight protons bound to the carbons of the two aromatic rings (quinolinone and phenyl), which have been assigned using $^1H—^1H$ gs-COSY and $^1H—^{13}C$ gs-HMQC experiments (Fig. 4). The singlet found at 11.98 ppm can be assigned to the proton at the nitrogen atom of quinoxalinone moiety in the position 1. The ^{13}C strong signals at 8.8 ppm and 46.7 ppm respectively, belong to the triethylammonium cation. The rest of the 15 carbon signals in the range of 118.8–172.9 ppm belong to the carbons forming the quinolinone and phenyl aromatic rings.

Table 2
Selected bond lengths (Å) and angles (°) for (Et_3NH) $[Zn(qui)Cl_2]$ and their comparison with complexes involving the $\{ZnO_2Cl_2\}$ chromophore, and deposited in Cambridge Structural Database.

Complex	d(Zn—O)/Å	d(Zn—Cl)/Å	∠(O—Zn—O)	∠(Cl—Zn—Cl)	Refs.
$[Zn(qui)Cl_2]$	1.9860(14)	2.2509(6)	85.12(6)	112.69(2)	This work
	1.9961(14)	2.2266(6)			
$[Zn(val)_2Cl_2]$	1.950(2)[a]	2.2430(7)[a]	91.77(9)	110.48(3)	ACETUX [34]
$[Zn(gly)_2Cl_2]$	1.9783(11)[a]	2.2314(3)[a]	97.79(4)	106.67(2)	AFEMEE [35]
$[Zn(dnb)_2Cl_2]^2$	1.949(3)	2.2552(13)	95.44(5)	113.26(4)	AVUHO [36]
	1.963(2)	2.2570(12)			
$[Zn(eaa)Cl_2]$	2.001(4)	2.213(2)	87.52(7)	117.52(6)	DIWLAW [37]
	2.008(3)	2.208(2)			
$[Zn(aed)Cl_2]$	1.957(5)	2.219(2)	88.4(2)	116.03(9)	NESDAR [38]
	1.976(5)	2.233(2)			
$[Zn(mqo)_2Cl_2]$	1.979(9)[a]	2.238(5)[a]	107.89(4)	120.43(2)	AFUSEZ [39]
$[Zn(gbp)_2Cl_2]$	1.959(2)	2.2517(9)	94.21(8)	110.56(3)	DOBBIG [40]
	1.985(2)	2.2580(10)			
$[Zn(H_2O)_2Cl_2]$	1.992(2)	2.195(2)	103.91(7)	125.12(8)	ELUCAQ [41]
	2.008(2)	2.197(2)			

List of abbreviations: *eaa* = *N,N′*-ethylene-acetylacetonimine, *aed* = (2-hydroxy-4-methoxy acetophenone)ethylenediamine, *val* = *D,L*-valine, *gly* = glycine, *mqo* = 2-methylquinoline *N*-oxide, *gbp* = gabapentine, *dnb* = 3,5-dinitrobenzoate.

[a] Only symmetrically independent bond lengths are displayed.

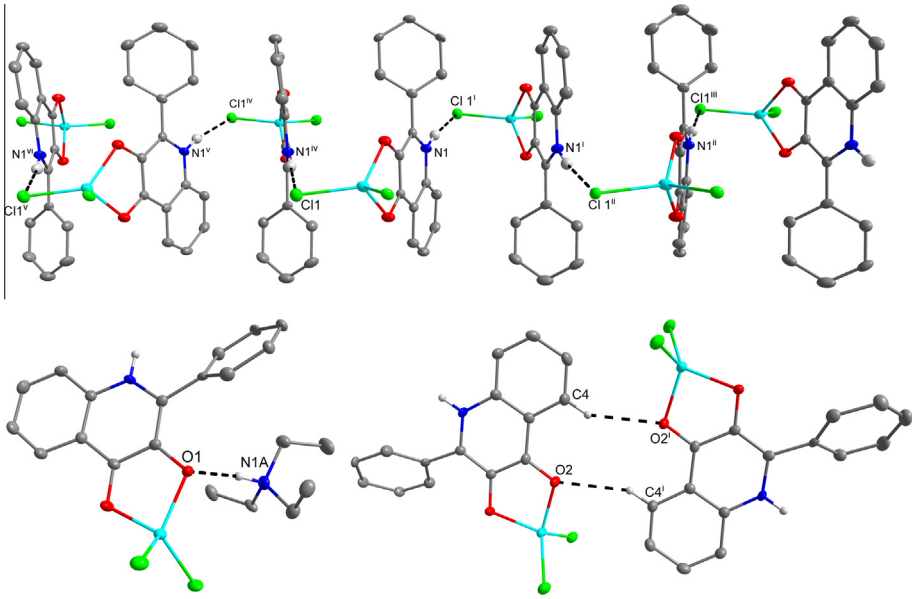

Fig. 2. A part of the crystal structure of (Et_3NH) [Zn(*qui*)Cl_2] showing non-covalent interactions. A perspective view on one-dimensional supramolecular substructure formed by N—H···Cl hydrogen bonding (*top*). Symmetry codes: (i) 1 − *x*, 0.5 + *y*, 1.5 − *z*; (ii) *x*, 1 + *y*, *z*; (iii) 1 − *x*, 1.5 + *y*, 1.5 − *z*; (iv) 1 − *x*, −0.5 + *y*, 1.5 − *z*; (v) *x*, −1 + *y*, *z*; (vi) 1 − x, −1.5 + *y*, 1.5 − *z*. The N—H···O hydrogen bond between the cation and complex anion (*down left*) and the C—H···O interactions between the complex anions (*down right*). The non-covalent contacts are displayed as black dashed lines. Hydrogen atoms (except for those involved in non-covalent interactions) are omitted for clarity.

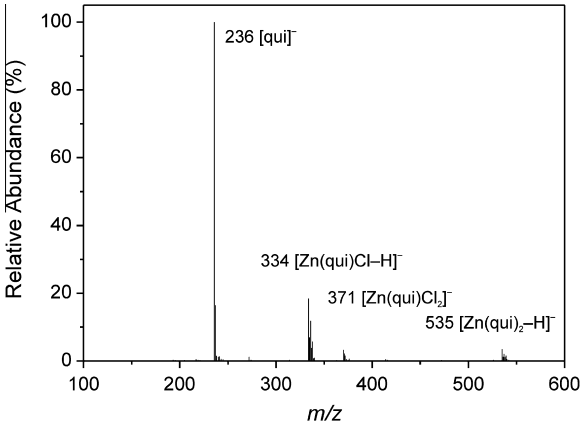

Fig. 3. ESI–MS spectrum of (Et_3NH) [Zn(*qui*)Cl_2], 10^{-5} M in methanol, showing the peak of the complex anion [Zn(*qui*)Cl_2]$^-$ and its fragmentation to [Zn(*qui*)Cl—H]$^-$ and [*qui*]$^-$ together with the recombination of the ligand and Zn(II), thus creating [Zn(*qui*)$_2$—H]$^-$.

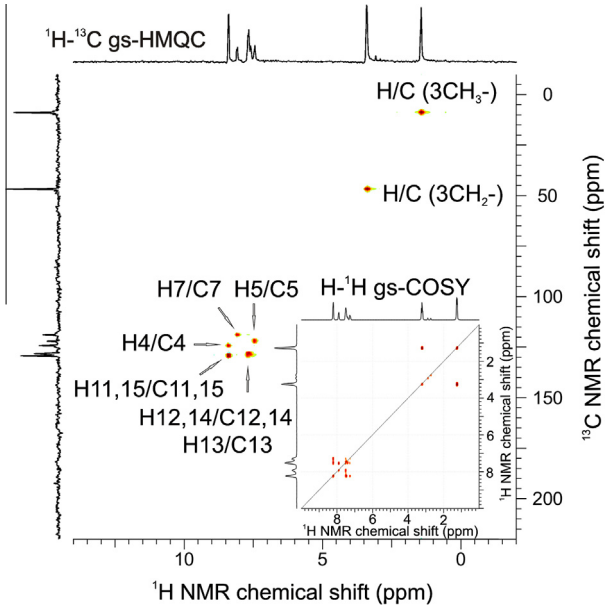

Fig. 4. ^{1}H—^{13}C gs-HMQC spectra (inset: ^{1}H—^{1}H gs-COSY spectra) of (Et_3NH) [Zn(*qui*)Cl_2].

3.4. UV absorption and fluorescence studies

The 10^{-4} M solution UV–vis absorption spectra were measured in order to find out the absorption maxima of each of the corresponding compounds, i.e. free H*qui*, (Et_3NH) [Zn(*qui*)Cl_2] and quinine sulfate as a standard (Fig. 5). The UV–vis spectrum of the free H*qui* ligand displays the absorption bands with maxima at 259 nm (ε = 10 270 M^{-1} cm^{-1}), 314 nm (ε = 1 660 M^{-1} cm^{-1}) and 362 nm (ε = 3590 M^{-1} cm^{-1}) from which the latter value was chosen as the excitation wavelength for subsequent fluorescent study. The bands associated with these maxima can be attributed to the π–π^* and/or n–π^* transitions. The (Et_3NH) [Zn(*qui*)Cl_2] complex shows very similar spectrum as compared with the free Hqui ligand, involving bands with the maxima at 268 (ε = 14 120 M^{-1} cm^{-1}), 312 nm (ε = 1 810 M^{-1} cm^{-1}) and 397 nm (ε = 4 720 M^{-1} cm^{-1}), however, especially the band centred at 397 nm, which was chosen as the excitation wavelength, is broadened and red-shifted. This feature may pointed out that the absorption may be associated with the coordination of the Hqui ligand to zinc and should not be ascribed to ligand-to-metal and/or metal-to-ligand charge transfer transitions.

To evaluate the fluorescence characteristics of (Et_3NH) [Zn(*qui*)Cl_2], the 10^{-4} M ethanolic solutions of the complex, quinine sulfate (standard) and free H*qui* ligand were measured at room temperature. Their fluorescence properties are depicted and compared in Fig. 5. It is shown that the complex displays one emission band centered at 477 nm (λ_{ex} = 397 nm) which is red-shifted as compared to that of free Hqui ligand with the maximum at 465 nm (λ_{ex} = 362 nm). In connection with these results it

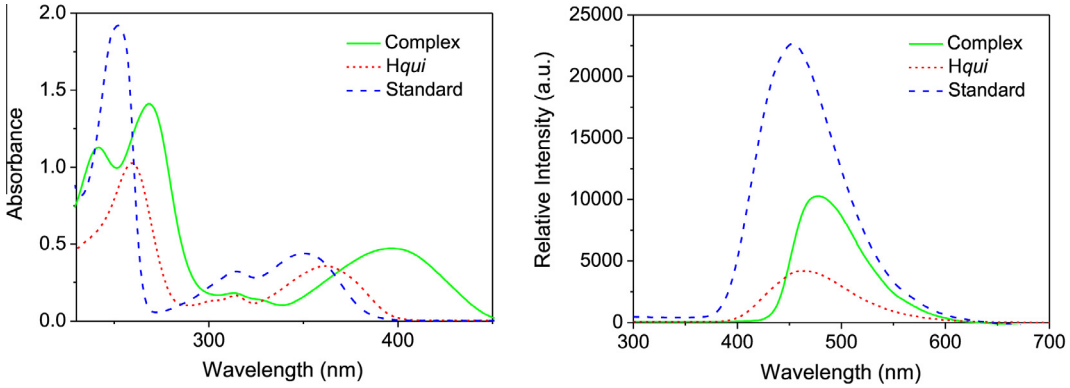

Fig. 5. Electronic absorption spectra (*left*) of the complex ($c = 1.0 \times 10^{-4}$ M) in ethanol (green full line) and H*qui* ($c = 1.0 \times 10^{-4}$ M) in ethanol (red dotted line), together with 1.0×10^{-4} M solution of the standard quinine sulfate in 0.1 M H_2SO_4 (blue dashed line). Part of fluorescence emission spectra (*right*) of the complex ($c = 1.0 \times 10^{-4}$ M) in ethanol (green full line) and H*qui* ($c = 1.0 \times 10^{-4}$ M) in ethanol (red dotted line) in comparison with the standard 1.0×10^{-4} M solution of quinine sulfate in 0.1 M H_2SO_4 (blue dashed line). (For interpretation of the references to color in this figure legend, the reader is referred to the web version of this article.)

may be proposed that the complex shows ligand-based fluorescence emission, which character may be associated with the π–π∗ and/or n–π∗ transitions of the coordinated qui ligand. The observed relative integral intensity of the complex and Hqui was found to be 29%, and 8.5%, respectively, of the intensity of the quinine sulfate used as a standard. On the other hand, the complex showed 1.6-fold enhancement of the emission with respect to free H*qui*.

3.5. In vitro cytotoxicity

Although the non-substituted 2-phenyl-3-hydroxy-4(1*H*)-quinolinone does not exhibit a relevant cytotoxic effect [8], we strived to find out how and/or whether the cytotoxicity could be affected by the coordination with biologically available zinc(II) atom. In order to find this out, we carried out *in vitro* cytotoxicity screening of (Et_3NH) [Zn(*qui*)Cl_2] against two human cancer cell lines (HOS and MCF7) and compared it with antitumor activity of *cisplatin* as a standard chemotherapeutic drug. Unfortunately, in spite of the fact that the complex was found to be well-soluble (>50.0 μM) in the medium used (0.1% DMF in a distilled water), and thus it should be quite well-bioavailable, the complex did not show any cytotoxic effect up to the 50.0 μM concentration. This means that the expectable IC_{50} values should lie above the value of IC_{50} = 50.0 μM, and generally speaking the compounds with such values of IC_{50} are considered to be inactive.

4. Conclusions

In summary, a novel zinc(II) quinolinone compound (Et_3NH)[Zn(*qui*)Cl_2] has been synthesized and characterized. The studied compound is actually the first Zn(II) complex with a ligand (*qui*) belonging to a large group of 2-phenyl-3-hydroxy quinolinones. The purity, composition and structure of the compound was evaluated on the basis of the results of elemental analysis, multinuclear (^{1}H, ^{13}C) and two-dimensional NMR spectroscopy, mass spectrometry and single-crystal X-ray analysis, which revealed a distorted tetrahedral coordination geometry of the {ZnO_2Cl_2} chromophore of the complex anion. The compound was tested on *in vitro* cytotoxicity against HOS and MCF7 cancer cell lines, and moreover the study of its fluorescence properties was also performed. The compound was found to be non-cytotoxic up to the concentration limit of 50.0 μM. The fluorescence study showed that the emission of (Et_3NH)[Zn(*qui*)Cl_2] is 1.6-times higher than that of free H*qui*.

Acknowledgements

This research was supported by the Operational Program Research and Development for Innovations – European Regional Development Fund (CZ.1.05/2.1.00/03.0058), Operational Program Education for Competitiveness – European Social Fund (CZ.1.07/2.3.00/20.0017) of the Ministry of Education, Youth and Sports of the Czech Republic and by Palacký University in Olomouc (PrF_2013_015). The authors would like to thank Dr. Michal Čajan for fluorescence measurements, Dr. Radka Křikavová for NMR experiments, Dr. Jana Gáliková for FT IR spectra, Mr. Tomáš Šilha for CHN analysis, and Prof. Zdeněk Dvořák for *in vitro* cytotoxicity testing.

References

[1] I. Otto, R. Gust, Arch. Pharm. 340 (2007) 117–126.
[2] M.J. Hannon, Pure Appl. Chem. 79 (2007) 2243–2261.
[3] M.A. Jakupec, M. Galanski, V.B. Arion, C.G. Hartinger, B.K. Keppler, Dalton Trans. 189 (2008) 183–194.
[4] S.H. van Rijt, P.J. Sadler, Drug Discov. Today 14 (2009) 1089–1097.
[5] G. Sava, A. Bergamo, P.J. Dyson, Dalton Trans. 40 (2011) 9069–9075.
[6] K.J. Kilpin, P.J. Dyson, Chem. Sci. 4 (2013) 1410–1419.
[7] R. Buchtík, Z. Trávníček, J. Vančo, R. Herchel, Z. Dvořák, Dalton Trans. 40 (2011) 9404–9412.
[8] R. Buchtík, Z. Trávníček, J. Vančo, J. Inorg. Biochem. 116 (2012) 163–171.
[9] Z. Trávníček, J. Vančo, J. Hošek, R. Buchtík, Z. Dvořák, Chem. Centr. J. 6 (2012) 160.
[10] Z. Sui, V.N. Nguyen, J. Altom, H. Jeffrey, J. Jamese, J.I. Bernstein, J.F. Barrett, K.A. Ohemeng, Eur. J. Med. Chem. 34 (1999) 381–387.
[11] Z. Sui, A. Jason, V.N. Nguyen, J. Fernandez, J.I. Bernstein, J.J. Hiliard, J.F. Barrett, B.L. Podlogar, K.A. Ohemeng, Bioorg. Med. Chem. 6 (1998) 735–742.
[12] P. Hradil, P. Krejčí, J. Hlaváč, I. Wiedermannová, A. Lyčka, V. Bertolasi, J. Heterocyclic Chem. 41 (2004) 375–379.
[13] D.A. Yushchenko, M.D. Bilokin, O.V. Pyvovarenko, G. Duportail, Y. Mély, G.V. Pivovarenko, Tetrahedron Lett. 47 (2006) 905–908.
[14] M.D. Bilokin, V.V. Shvadchak, D.A. Yushchenko, A.S. Klymchenko, G. Duportail, Y. Mély, G.V. Pivovarenko, Tetrahedron Lett. 50 (2009) 4714–4719.
[15] Y. Mikata, Y. Sato, S. Takeuchi, Y. Kuroda, H. Konno, S. Iwatsuki, Dalton Trans. 42 (2013) 9688.
[16] J.M. Berg, Y. Shi, Science 271 (1996) 1081–1085.
[17] Z. Wu, Y. Zhang, J.S. Ma, G. Yang, Inorg. Chem. 45 (2006) 3140–3142.
[18] A.C. Miu, O. Benga, P.A. Adlard, A.I. Bush, J. Alzheimer's Dis. 10 (2006) 145–163.
[19] E.L. Que, D.W. Domaille, C.J. Chang, Chem. Rev. 108 (2008) 1517–1549.
[20] G. Barone, A. Terenzi, A. Lauria, A.M. Almerico, J.M. Leal, N. Busto, B. García, Coord. Chem. Rev. (2013). doi:/10.1016/j.ccr.2013.02.023.
[21] X. Zhou, B. Yu, Y. Guo, X. Tang, H. Zhang, W. Liu, Inorg. Chem. 49 (2010) 4002–4007.
[22] Z.K. Song, B. Dong, G.J. Lei, M.J. Peng, Y. Guo, Tetrahedron Lett. 54 (2013) 4945–4949.
[23] Z. Trávníček, V. Kryštof, M. Šipl, J. Inorg. Biochem. 100 (2006) 214–225.
[24] Q. Jiang, J. Zhu, Y. Zhang, N. Xiao, Z. Guo, Biometals 22 (2009) 297–305.
[25] J. Hošek, R. Novotná, P. Babula, J. Vančo, Z. Trávníček, PLOS ONE 8 (2013) e65214.

[26] K.W. Tan, H.L. Seng, F.S. Lim, S.C. Cheah, C.H. Ng, K.S. Koo, M.R. Mustafa, S.W. Ng, M.J. Maah, Polyhedron 38 (2012) 275–284.
[27] P.F. Liguori, A. Valentini, M. Palma, A. Bellusci, S. Bernardini, M. Ghedini, M.L. Panno, C. Pettinari, F. Marchetti, A. Crispini, D. Pucci, Dalton Trans. 39 (2010) 4205–4212.
[28] P. Hradil, J. Jirman, Collect. Czech Chem. Commun. 60 (1995) 1357–1366.
[29] W.H. Melhuish, J. Phys. Chem. 65 (1961) 229–235.
[30] CrysAlis CCD and CrysAlis RED, Version 1.171.33.52, Oxford Diffraction Ltd., England, 2009.
[31] M. Sheldrick, Acta Crystallogr. A: Found Crystallogr. 64 (2008) 112–122.
[32] K. Brandenburg, DIAMOND, Release 3.1f, Crystal Impact GbR, Bonn, Germany, 2006.
[33] W.J. Geary, Coord. Chem. Rev. 7 (1971) 81–122.
[34] M.S. Nandhini, R.V. Krishnakumar, S. Natarajan, Sect. E: Struct. Rep. Online 57 (2001) m498–m500.
[35] S.M.N. Priya, B. Varghese, J.M. Linet, S.J. Das, Sect. E: Struct. Rep. Online 63 (2007) m2318.
[36] E.B. Miminoshvili, A.N. Sobolev, K.E. Miminoshvili, T.N. Sakvarelidze, Acta Crystallogr. Sect. E 60 (2004) m319–m321.
[37] V.S. Velezheva, A.I. Sokolov, A.G. Kornienko, K.A. Lyssenko, Y.V. Nelyubina, I.A. Godovikov, A.S. Peregudov, A.F. Mironov, Tetrahedron Lett. 49 (2008) 7106–7109.
[38] Z.M. Zhang, D.Q. Wang, G. Jian, S. Li, Sect. E: Struct. Rep. Online 62 (2006) m3570–m3572.
[39] S.N. Ivashevskaja, L.A. Aleshina, V.P. Andreev, Y.P. Nizhnik, V.V. Chernyshev, H. Schenk, Sect. C: Cryst. Struct. Commun. 58 (2002) m300–m301.
[40] D. Braga, F. Grepioni, L. Maini, R. Brescello, L. Cotarca, CrystEngComm 10 (2008) 469–471.
[41] Y.V. Kokunov, Y.E. Gorbunova, V.V. Kovalev, Russ. J. Inorg. Chem. 54 (2009) 1603–1610.
[42] C.J. Pouchert, The Aldrich Library of infrared Spectra, Third ed., Aldrich, Milwaukee, 1981.
[43] T. Beringhelli, M. Freni, F. Morazzoni, P. Romiti, R. Servida, Spectrochim. Acta 37A (1981) 763–771.
[44] R. Novotná, I. Popa, Z. Trávníček, Inorg. Chim. Acta 365 (2011) 113–118.
[45] G. Socrates, Infrared and Raman Characteristic Group Frequencies, Third ed., Wiley, Chichester, 2004.